

Journal of Materials Chemistry A

Accepted Manuscript



This is an *Accepted Manuscript*, which has been through the Royal Society of Chemistry peer review process and has been accepted for publication.

Accepted Manuscripts are published online shortly after acceptance, before technical editing, formatting and proof reading. Using this free service, authors can make their results available to the community, in citable form, before we publish the edited article. We will replace this *Accepted Manuscript* with the edited and formatted *Advance Article* as soon as it is available.

You can find more information about *Accepted Manuscripts* in the [Information for Authors](#).

Please note that technical editing may introduce minor changes to the text and/or graphics, which may alter content. The journal's standard [Terms & Conditions](#) and the [Ethical guidelines](#) still apply. In no event shall the Royal Society of Chemistry be held responsible for any errors or omissions in this *Accepted Manuscript* or any consequences arising from the use of any information it contains.

Low electric field strength self-organization of anodic TiO₂ nanotubes in diethylene glycol electrolyte

Cite this: DOI: 10.1039/x0xx00000x

Damian Kowalski,^{*a,b} Jeremy Mallet^a, Jean Michel^a and Michael Molinari^a

Received 00th January 2012,
Accepted 00th January 2012

DOI: 10.1039/x0xx00000x

www.rsc.org/

Self-organization of TiO₂ nanotubes with large interconnecting space in-between tubes has been demonstrated by means of anodizing of titanium in diethylene-glycol/HF electrolyte containing desired content of water. The unique morphological features are a consequence of low electric field strength conditions leading to growth of tubes on low population of nucleation sites. The proposed growth model assumes the presence of metallic titanium in-between the tube cells which is oxidized/etched resulting in generation of inhomogeneous oxide at the bottom of nanostructure. The presented work makes a contribution to the research field in few aspects: i) the low field strength conditions have been demonstrated to have an impact on the tubes spacing, ii) the water content in electrolyte allows precise control of the interconnecting space in-between the tubes, iii) the tubes separation is controlled by the presence of Ti in-between the tube cells.

Introduction

The anodizing is a high-voltage electrochemical conversion process that forms barrier-type oxide layers or nanoporous/nanotubular structures on valve metals and alloys mainly depending on the composition of electrolyte used.^{1, 2} The key to achieve the ordered nanoporous/nanotubular structures is a displacement of the film material above the original surface position due to synergistic effect of pits generation (field assisted oxide dissolution), stress generated at the metal-oxide interface including electrostriction³⁻⁵ together with plastic oxide flow⁶⁻¹⁰ switching the growth of the barrier-film to nanotube/nanopore.

The first recognized works on formation of nanotubes on titanium (Assefpour-Dezfuly)¹¹ and nanopores on Ti and TiAl alloy (Zwilling et al.)^{12, 13} demonstrated low voltage synthesis, up to 10V, in chromic acid electrolytes containing fluorides. The further works (Gong et al.)¹⁴ extended the synthesis voltage to tens of volts demonstrating a clear shape of TiO₂ nanotubes and establishing a specific action of fluorides in water based electrolytes. The further advance in the synthesis of nanotubes was done by Macak et al.¹⁵ by introduction of organic electrolytes in which long and smooth TiO₂ nanotubes could be formed.

Typically, the TiO₂ nanotube array formed in organic electrolytes such as glycerol,¹⁵ dimethyl sulfoxide,¹⁶ ethylene-glycol,¹⁷ is obtained in the form of close packed structure in which the nanotubes nearly stick together with the tube walls. A fundamentally different nanostructure from that is obtained in diethylene-glycol electrolyte initially reported by Yoriya et al.¹⁸⁻²¹ The nanostructure is characterized by free standing nanotubes separated by an interconnecting space larger than the diameter of nanotubes. Although, many aspects for the tubes growth, such as field assisted dissolution, volume expansion, stress generated at metal/oxide interface, electrostriction, plastic

oxide flow proposed in the growth models for alumina and titania^{2, 7, 9, 22-26} may hold for formation of the tubes, the reason for formation of large spacing is not well understood. Herein we shine a light on how the tubes are formed with large interconnecting space in between which allows us to better understand the self-ordering process in anodizing of titanium.

Results and discussion

Figure 1 shows SEM image for TiO₂ nanotubes which were synthesised by means of anodizing of titanium at 70 V for 16h in diethylene-glycol electrolyte containing 2 wt.% HF and 2 wt.% H₂O. The nanotubes are characterized by relatively large interconnecting space in-between nanotubes in comparison with classic TiO₂ nanotubes.²⁷ In order to control the free space in-between nanotubes, one possibility is to modify composition of anodizing electrolyte by playing with water content.^{28, 29} Figure 2 shows the nanostructures obtained by anodizing of Ti at 60V

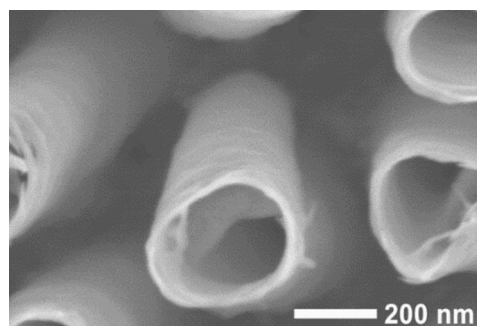


Fig. 1 The SEM top view for TiO₂ nanotubes with large interconnecting space in-between the tubes; the nanostructure was synthesised by anodizing of Ti at 70V for 16h in diethylene glycol electrolyte containing 2 wt.% HF and 2 wt.% H₂O.

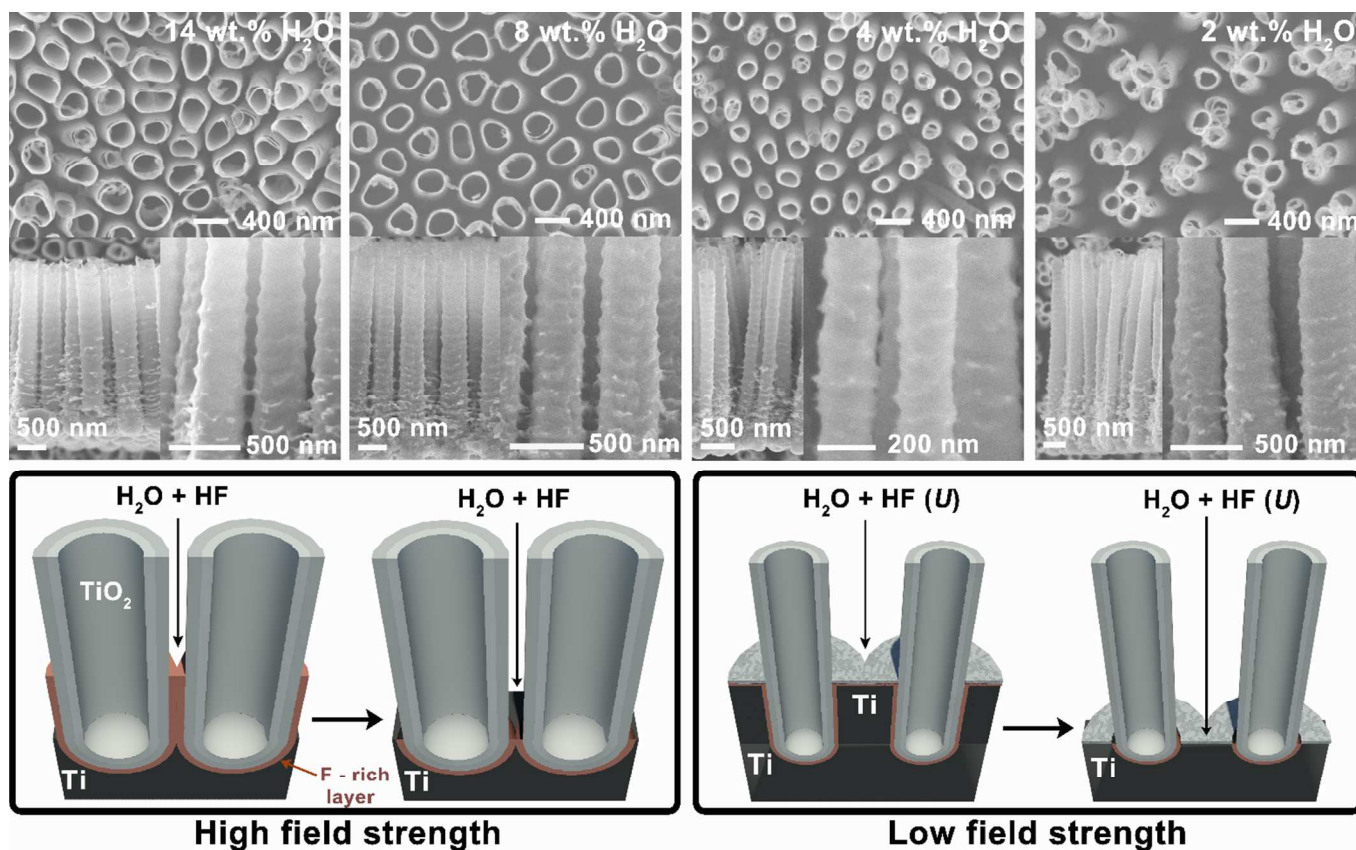


Fig. 2 SEM top and cross-section views for TiO₂ nanotubes formed at 60V for 16h in diethylene glycol electrolyte containing water content from 2-14 wt.%. The high-electric-field model assuming formation of space in-between the tubes by dissolution of fluoride rich layers, *i.e.* TiF_x, TiF_xO_y or similar (bottom left). The low electric-field-model assuming generation of tubes of small diameter on low population of nucleation sites; the titanium is present in-between the bottom tube cells (bottom right).

for 16h in diethylene-glycol electrolyte containing 2 wt.% HF and water content from 12 to 2 wt.%. From the SEM micrographs it is obvious that the water content has significant impact on the growth of nanotubes and resulting morphology of the nanostructures. The nanotubes formed in high H₂O content (Fig. 2 top left) are of relatively large diameter (*ca.* 340nm) with interconnecting space in-between the tubes approaching 100nm. Reduction of H₂O content in electrolyte to 2 wt.% results in increase of interconnecting space to 320nm and decrease of the tube diameter to 185nm (Fig. 2 top right). At this point the space in-between nanotubes is larger than their diameter and some agglomeration of the tubes can be observed. This is due to the tendency of the tubes to stick together due to surface tension forces acting on each nanotube during drying process.³⁰ Such relatively large space in-between the tubes is unusual for titanium anodized in classic organic electrolytes. Together with the decrease of tube diameter there is a slight reduction of the tube wall thickness from 20 nm to 12 nm for 340nm and 185nm tubes, respectively. The interconnecting space in-between the nanotubes, nanotube diameter and wall thickness linearly change with water content in electrolyte, as demonstrated in Fig. 3. The length of nanotubes formed in diethylene glycol is 3-4 μm, which means that the kinetics of dissolution in electrolyte containing small water content is already fast comparing with other organic electrolytes such as glycerol¹⁵ and dimethyl sulfoxide¹⁶. No significant influence of water content on the length of nanotubes has been found.

Anodic oxide is known to grow by simultaneous migration of cations towards the metal/oxide interface and anions towards the oxide/electrolyte interface by a cooperative mechanism, forming oxide both at the metal/oxide and at the oxide/electrolyte interfaces.^{31, 32} The degree of complexity for anodizing process is rather high and many parameters such as current/potential, water content, fluoride ions concentration as well as pH of electrolyte have a strong impact on the oxide growth. Some of those aspects have been reviewed in²⁷. Herein we particularly discuss on the parameters affecting electric field strength.

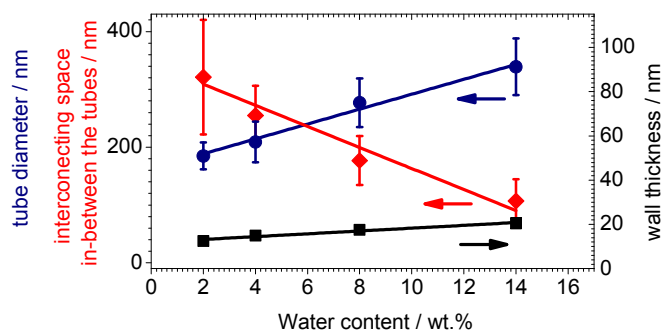


Fig. 3 The size of interconnecting space in-between nanotubes, outer nanotube diameter and wall thickness as a function of water content in electrolyte.

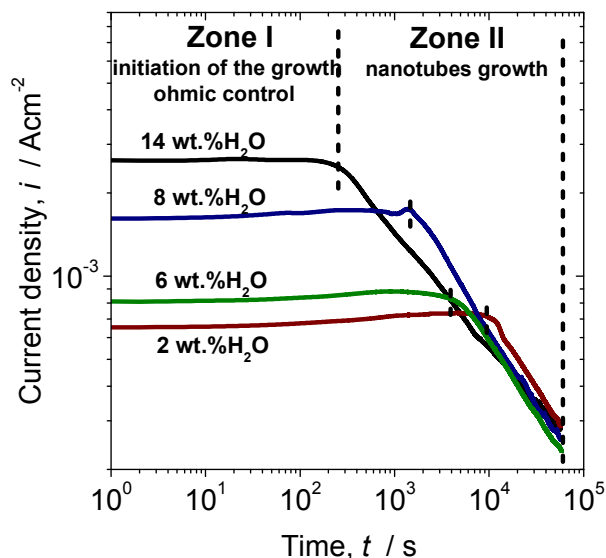


Fig. 4 Double logarithmic $i-t$ plot for anodizing of titanium at 60V in diethylene glycol electrolyte containing 2 wt.% HF and water content 2-14 wt.%.

The change in the growth mechanism is obvious when we have a look at the anodizing current-time ($i-t$) with an exponential function for both current and time (Fig. 4). Two linear current regions can be clearly recognized in the double logarithmic $i-t$ graph: i) the region with slightly positive slope, and ii) the region with negative slope in which the logarithm of current linearly drops with logarithm of time. The zone I is most likely associated with the initial growth of the barrier-type oxide layer with thickness of tens of nanometers, followed by simultaneous dissolution and growth of that layer. At this point, the population of nucleation sites for the tubes growth is established. In the zone II the growth of nanotubes, is accompanied by electrochemical etching of the top of nanostructure. Taking into account the logarithmic scale the $i-t$ profile is comparable to those observed for other organic electrolytes^{16, 33, 34} even if Yoriya et al. have observed an increase of the current density with anodizing time.¹⁸ These differences may be explained different geometry of the electrochemical cells leading to variations in oxide formation/dissolution kinetics.

The zone I, in which the barrier layer is formed, is significantly extended from 200s to 3h when the water content in electrolyte is reduced from 12 wt.% to 2 wt.%, respectively. For the anodizing in classic organic electrolytes (e.g. dimethyl sulfoxide, ethylene glycol, glycerol) the time necessary to initiate nanotubes growth usually does not exceed hundreds of seconds. One may also notice a considerable change of current density for the nucleation of the pores; $\log i$ is four times bigger for tubes formed in electrolyte containing 14 wt.% H₂O than that formed in 2 wt.% H₂O which is in agreement with increase of electrolyte conductivity.²⁰

To explain the mechanism of nanotubes formation let us first consider what happens at the very beginning of anodizing process. At first, it should be noted here that anodizing in organic electrolytes results in significant ohmic drop (IR_{Ω} drop³⁵) due to relatively low conductivity of electrolytes. What is very often overlooked in the literature is the effect of reaction (1) at oxide/electrolyte interface which results in injection of Ti species

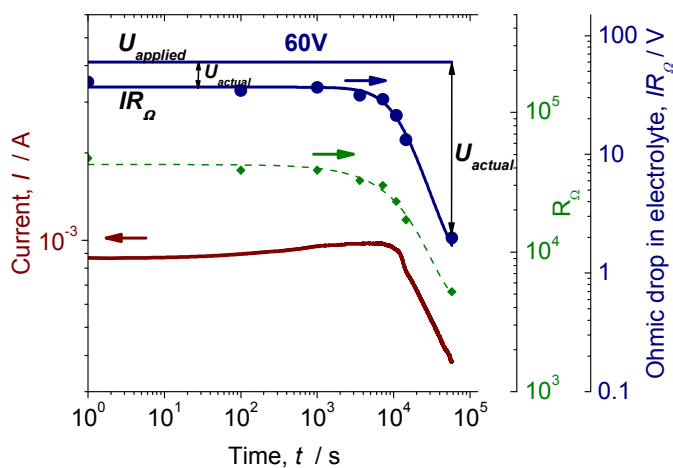
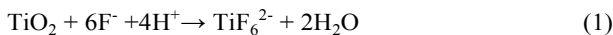


Fig. 5 The ohmic drop in electrolyte during anodizing of titanium in diethylene glycol, 2 wt.% HF 2 wt.% H₂O.

to electrolyte, strongly modifying its composition and therefore electrolyte conductivity.



It simply means that the anodizing conditions are changing with anodizing time. For the low concentrated ternary H₂TiF₆ + HF + H₂O systems the conductivity of electrolyte has been shown to increase with the TiF₆²⁻ content.³⁶ Although, there is no literature information about conductivity mechanism for such system in the presence of diethylene glycol, our results show similar trend. Figure 5 shows AC impedance measured between counter and working electrodes for anodizing of titanium at 60V in electrolyte containing 2 wt.% HF and 2 wt.% H₂O. The resistance of fresh electrolyte is as high as 50 kΩ, and calculated ohmic drop between counter and working electrodes is 45 V. It means that by applying 60 V, most of the voltage is consumed for IR_{Ω} compensation and therefore effective voltage for oxide development at the beginning of anodizing (zone I) is only 15 V. Such radical change of voltage strongly affects the growth mechanism. With the time of anodizing the conductivity of electrolyte increases according to reaction (1) consequently reducing the ohmic drop. After 16h of anodizing the resistance of electrolyte drops to 14 kΩ and calculated ohmic drop is equal to only 7 V. One important conclusion arises from this experiment: the electric-field-strength which is defined as:

$$E = (U_{\text{applied}} - IR_{\Omega}) / d \quad (1)$$

(E / Vm^{-1} is an electric field strength, U / V applied voltage, IR_{Ω} ohmic drop, d / m thickness of oxide layer) is significantly lowered at the beginning of anodizing process due to the massive effect of ohmic drop.

Under slowly released Ti species, at the oxide/electrolyte interface, the electric-field-strength is essentially controlled by ohmic drop in electrolyte. Two assumptions can be formulated: i) the growth of the nanotubes cannot proceed until certain value of E is reached over initially formed barrier-layer. This can be clearly seen on the anodizing curve where initial growth zone is extended to 3h for electrolyte in which high ohmic drop is observed, ii) the lower field strength conditions are established at low $\log i$.

For the classic theory of ionic conduction at the high electric-field-strength, the logarithm of current density, $\log i$, is inversely proportional to the thickness of oxide, *i.e.* proportional to electric-field-strength at the barrier layer.³⁷ The effect of electric-field-strength on self-organization of pores has been demonstrated in detail by Ono et al.³⁸ for anodic alumina. The high-field-strength self-organization has been established at current density close to the burning current of 50 mAcm^{-2} ,³⁸ and $30\text{--}250 \text{ mAcm}^{-2}$ ³⁹ for hard anodizing. For anodic titania the current densities as high as 100 mAcm^{-2} ,⁴⁰ 150 mAcm^{-2} ⁴¹ were reported for close packed nanotubes. It is therefore not surprising to observe lowered electric-field-strength conditions at current density of 0.6 mAcm^{-2} in Fig.4.

It is generally accepted that lower E would produce lower diameter of the pore/nanotube. The diameter of nanotubes in Fig. 2 is reduced from 340nm to 185nm for the anodizing with water content from 14 % to 2 %, respectively. This is in agreement with $\log i$ values observed in zone I in Fig. 4.

By looking at the SEM images in Fig. 2 one may find one important detail; the number of tubes, *i.e.* population of the pores in which the tubes are formed, is approximately the same for all anodizing conditions. What makes the difference in nanostructures is the diameter of the tubes which are formed under different strength conditions; smaller diameter for the low $\log i$, *i.e.* lower electric-field-strength conditions, large tube diameter under high $\log i$, *i.e.* higher electric-field-strength conditions.

To verify the field effect on separation of the nanotubes we have tried to decrease the electric-field-strength even further by means of manipulation at the anodizing voltage (Eq.1). Figure 6 shows SEM image of the nanotubes formed at 40V for 16h. The formed space in-between the tubes is so large that the tubes have tendency to agglomerate during drying process resulting in collapse of nanostructure. This result confirms the electric-field-strength effect on nanotubes separation.

The scheme in Fig. 2 (bottom left) shows presently accepted model for the titania nanotubes growth which assumes formation of fluoride rich layer in between the tubes.^{25, 34} The fluoride rich layer has been shown to be formed at metal/oxide interface due to competitive inward migration of fluoride ions towards oxygen with the thickness of the layer approximately 10-20% of formed oxide.^{42, 43} The structure of fluoride rich layer (TiF_x , TiF_xO_y or

similar) is not clear in the literature and there is no evidence on its chemical nature.^{42, 44} During the formation process, the nanotubes stick together with fluoride rich layers forming initial nanoporous cell.^{25, 44} The fluoride rich layer is then dissolved in electrolyte, possibly forming TiF_6^{2-} or oxy-hydroxy analogous of this compound. The layers which connect the tubes are dissolved and the native porous character is turned into nanotubular one (Fig.2 bottom left). The space in between nanotubes is then approximately equal to double thickness of fluoride rich layer. The thickness of the tube wall measured at the bottom of nanostructure is 72nm which means that for the tubes grown under high electric-field-strength the calculated theoretical interconnecting distance in-between nanotubes would be *c.a.* $2 \times 16 \text{ nm}$.

The distance measured in-between nanotubes in Fig. 2 and 3 is 320nm giving 170nm distance for fluoride rich layer, which is as much as 10 times thicker than the possible theoretical value. Since the measured distance much exceeds the thickness of oxide formed at the barrier layer, the formation of fluoride rich layer cannot explain such big interconnecting space in-between nanotubes, and the missing material from the space in-between nanotubes must be found.

Figure 2 (bottom right) shows possible mechanism of the tubes growth which considers additional titanium metal layer which is located in-between the tubes under anodizing on low population of nucleation sites, under low electric-field-strength conditions (low $\log i$), resulting in large separation of the individual tubes. During the tubes growth the metallic form of titanium is located in between the tube cells. The oxidation of the interconnecting titanium may be analogous to formation of barrier-layer containing voids, cavities and cracks⁴⁵ leading to non-uniform field distribution and formation of meso/nano porosity. Some etching by penetrating electrolyte may also play a role.^{46, 47} By looking at the cross-section in Fig. 2 one may find inhomogeneous material in the lower parts of titania nanotubes which supports that concept.

To confirm that mechanism we carefully analyzed the bottom side of nanotubes. In Fig. 7 the tube bottoms are separated by large interconnecting space. We would like to emphasize here the very unique observation for the bottom side of titania: the formed tubes cells (bottoms) are disconnected and this must be caused by presence of titanium metal in-between the bottom cells

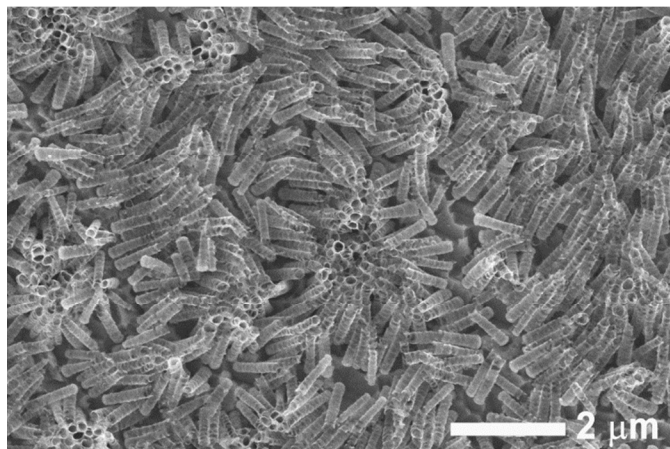


Fig. 6 TiO_2 nanotubes obtained by lowering the electric field strength by means of manipulation at applied voltage. Ti was anodized at 40V in diethylene glycol (2 wt.% HF 2 wt.% H_2O).

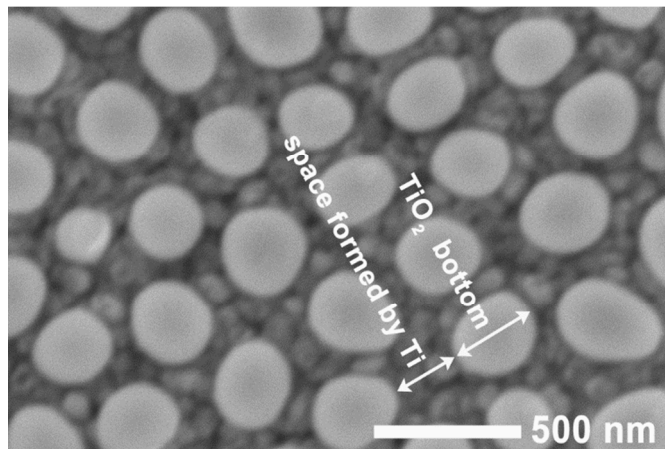


Fig. 7 The bottom side of titania nanotubes. Titanium was anodized at 60V for 16h in diethylene glycol, 2 wt.% HF, 2 wt.% H_2O .

during the growth. Such mechanism is possible since the tubes grow mainly downward due to continuous electrochemical etching of the top of nanostructure during anodizing. Titanium which is initially located below the oxide metal interface becomes located in-between the tubes cells. At this point one may consider rather different kinetics for the oxidation of metal in between the tubes due to competition between growth of nanotube and oxidation of titanium in-between. An inhomogeneous material can be found in-between the tube bottoms in Fig. 7. The origin of that material is the product of oxidation/etching (discussed below). The above observations allow us to conclude that the distance in-between nanotubes is formed of two fluoride rich layers located at the outer shell of tubes and large fraction of titanium metal in-between them Fig. 2 (bottom right). Another crucial point is that the tube bottoms are more randomly distributed which is characteristic for low field-strength effect.³⁸

Figure 8 shows TEM micrograph for TiO₂ nanotube formed in diethylene glycol electrolyte containing 2 wt.% water and 2 wt.% HF. The “V” shape of 3.3 μm long nanotube is clearly observed inside the tube; the outer diameter of the tube is 230nm, the inner one is 200nm and 140nm at top and bottom, respectively. The XRD and TEM analysis show amorphous structure for titania nanotubes, however the high-resolution TEM micrograph for the inhomogeneous material attached to nanotube wall show many small crystalline regions with lattice fringes of 2.1 Å as those shown in Fig. 8. Since the material in-between the tubes grows with not well defined protocol the possible explanation of the nanocrystals formation is oxygen generation within the framework of inhomogeneous oxide.⁴⁵ The lattice fringes of 2.1 Å cannot be indexed to common TiO₂ phases such as rutile and anatase and may be due to the existence of titanium ions of intermediate oxidation state such as TiO (PDF 00-008-0117).

The obtained nanostructures may find applications in the composite systems or as a templates for electrodeposited structures in view of very unique deposition pathways in anodic titania.^{29, 48-50}

Experimental

Titania nanotubes were formed by anodizing of 0.1 mm thick titanium foils of 99.6% purity purchased from GoodFellow.

Before use, titanium specimens were degreased by sonication in acetone and ethanol, rinsed in deionized Milli-Q water and dried in a nitrogen stream. The foils were anodized in diethylene glycol electrolyte containing 2 wt.% HF (50%) and desired amount of water. It should be noted here that addition of 2 wt.% HF already gives 2 wt.% of water in the electrolyte. Herein the described amount of water is a sum of added pure water, and water added with HF. Anodizing was carried out in cylindrical two-electrode Teflon cell with platinum counter electrode. The distance between working and counter electrodes was kept constant at 14mm. The geometrical surface of the titanium working electrode was 1.327 cm². The small volume of electrolyte was used (3cm³) to quickly adjust the electrolyte composition during anodizing (Ti dissolution). The temperature of electrolyte was 22±1 °C. After synthesis step the anodized titanium sample was immersed in acetone for 30min and left in air for drying.

The anodizing of titanium was carried out by constant potential protocol using a HP 6209B DC power supply connected to Fluke 45 digital multimeter. The impedance measurements were performed in two electrode system using VOLTALAB

PGZ301 at open circuit potential in the frequency range 100kHz-1Hz with

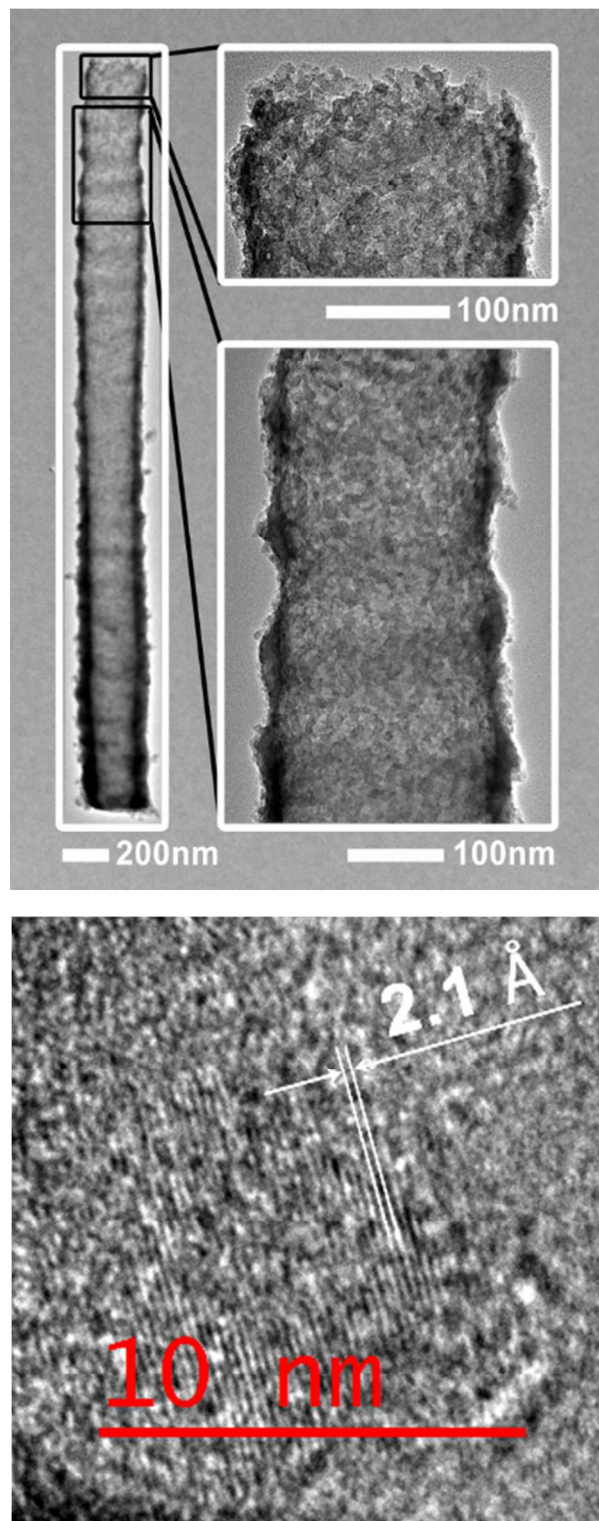


Fig. 8 Transmission electron microscopy images for TiO₂ synthesized in diethylene glycol, 2 wt.% HF, 2 wt.%H₂O at 60V for 16h. The micrograph at the bottom shows high resolution image for the inhomogeneous parts attached to nanotube wall.

the AC amplitude of perturbation signal 10mV. The measurements of electrolyte impedance during the anodizing were performed in parallel cell in which titanium working electrode was replaced with gold electrode.

A field emission scanning electron microscope (FE-SEM, LEO GEMINI) was used for structural and morphological characterization of titania nanotubes. Transmission electron microscopy (TEM) characterization was performed using a field emission JEOL 2100F microscope operating at 200kV. TEM micrographs were recorded using a GIF quantum CCD sensor.

Conclusion

The anodizing of titanium in diethylene glycol electrolyte results in formation of the titania nanotubes which are separated with interconnecting space exceeding the diameter of nanotubes. The size in-between the tubes was controlled by water content in electrolyte. It was demonstrated that the low electric-field-strength conditions (low $\log i$) in the initiation of the nanotube growth have a huge impact on the growth mechanism. The analysis of the tubes bottoms showed that the tubes grow individually, separated by a fraction of titanium metal in between the bottom tube cells. The presence of ohmic drop (IR_{Ω}) in electrolyte has significant influence on titania growth and should be taken into consideration in anodizing process.

Acknowledgements

The authors would like to acknowledge Laurence Wortham for TEM studies and PICT and NanoMat Platforms of the University of Reims Champagne Ardenne for access to the TEM. D.K. would like to acknowledge for financial support from National Science Centre grant number 2013/11/B/ST4/02151.

Notes and references

^a Laboratoire de Recherche en Nanosciences, LRN EA4682, University of Reims Champagne-Ardenne, Campus Moulin de la Housse, BP 1039, 51687 Reims, France.

damian.kowalski@univ-reims.fr

^b University of Warsaw, Faculty of Chemistry, Pasteura 1, 02-093 Warsaw Poland.

- H. Masuda and K. Fukuda, *Science*, 1995, **268**, 1466-1468.
- G. E. Thompson, R. C. Furneaux, G. C. Wood, J. A. Richardson and J. S. Goode, *Nature*, 1978, **272**, 433-435.
- N. Sato, *Electrochim Acta*, 1971, **16**, 1683-1692.
- K. Nielsch, J. Choi, K. Schwirn, R. B. Wehrspohn and U. Gosele, *Nano Lett*, 2002, **2**, 677-680.
- S. J. Garcia-Vergara, P. Skeldon, G. E. Thompson and H. Habazaki, *Corros Sci*, 2007, **49**, 3772-3782.
- P. Skeldon, G. E. Thompson, S. J. Garcia-Vergara, L. Iglesias-Rubianes and C. E. Blanco-Pinzon, *Electrochim Solid St*, 2006, **9**, B47-B51.
- S. J. Garcia-Vergara, P. Skeldon, G. E. Thompson and H. Habazaki, *Electrochim Acta*, 2006, **52**, 681-687.
- S. J. Garcia-Vergara, P. Skeldon, G. E. Thompson and H. Habazaki, *Appl Surf Sci*, 2007, **254**, 1534-1542.
- J. E. Houser and K. R. Hebert, *Nat Mater*, 2009, **8**, 415-420.
- S. J. Garcia-Vergara, P. Skeldon, G. E. Thompson, T. Hashimoto and H. Habazaki, *J Electrochem Soc*, 2007, **154**, C540-C545.
- M. Assefpour-Dezfuly, C. Vlachos and E. H. Andrews, *J Mater Sci*, 1984, **19**, 3626-3639.
- V. Zwillling, E. Darque-Ceretti, A. Boutry-Forveille, D. David, M. Y. Perrin and M. Aucouturier, *Surface and Interface Analysis*, 1999, **27**, 629-637.
- V. Zwillling, M. Aucouturier and E. Darque-Ceretti, *Electrochim Acta*, 1999, **45**, 921-929.
- D. Gong, C. A. Grimes, O. K. Varghese, W. C. Hu, R. S. Singh, Z. Chen and E. C. Dickey, *J Mater Res*, 2001, **16**, 3331-3334.
- J. M. Macak, H. Tsuchiya, L. Taveira, S. Aldabergerova and P. Schmuki, *Angewandte Chemie-International Edition*, 2005, **44**, 7463-7465.
- M. Paulose, K. Shankar, S. Yoriya, H. E. Prakasam, O. K. Varghese, G. K. Mor, T. A. Latempa, A. Fitzgerald and C. A. Grimes, *J Phys Chem B*, 2006, **110**, 16179-16184.
- S. P. Albu, A. Ghicov, J. M. Macak, R. Hahn and P. Schmuki, *Nano Lett*, 2007, **7**, 1286-1289.
- S. Yoriya, G. K. Mor, S. Sharma and C. A. Grimes, *J Mater Chem*, 2008, **18**, 3332-3336.
- S. Yoriya and C. A. Grimes, *Langmuir*, 2009, **26**, 417-420.
- S. Yoriya and C. A. Grimes, *J Mater Chem*, 2011, **21**, 102-108.
- S. Yoriya, *International Journal of Electrochemical Science*, 2012, **7**, 9454-9464.
- G. E. Thompson, K. Shimizu and G. C. Wood, *Nature*, 1980, **286**, 471-472.
- G. E. Thompson and G. C. Wood, *Nature*, 1981, **290**, 230-232.
- O. Jessensky, F. Muller and U. Gosele, *Appl Phys Lett*, 1998, **72**, 1173-1175.
- A. Valota, D. J. LeClere, P. Skeldon, M. Curioni, T. Hashimoto, S. Berger, J. Kunze, P. Schmuki and G. E. Thompson, *Electrochim Acta*, 2009, **54**, 4321-4327.
- Z. Su and W. Zhou, *Advanced Materials*, 2008, **20**, 3663-3667.
- D. Kowalski, D. Kim and P. Schmuki, *Nano Today*, 2013, **8**, 235-264.
- J. M. Macak, H. Hildebrand, U. Marten-Jahns and P. Schmuki, *J Electroanal Chem*, 2008, **621**, 254-266.
- D. Kowalski, A. Tighineanu and P. Schmuki, *J Mater Chem*, 2011, **21**, 17909-17915.
- J. J. Hill, K. Haller, B. Gelfand and K. J. Ziegler, *ACS Appl Mater Inter*, 2010, **2**, 1992-1998.
- J. P. S. Pringle, *Electrochim Acta*, 1980, **25**, 1403-1421.
- J. P. S. Pringle, *Electrochim Acta*, 1980, **25**, 1423-1437.
- J. M. Macak, H. Tsuchiya, A. Ghicov, K. Yasuda, R. Hahn, S. Bauer and P. Schmuki, *Curr Opin Solid St M*, 2007, **11**, 3-18.
- S. Berger, J. Kunze, P. Schmuki, A. T. Valota, D. J. LeClere, P. Skeldon and G. E. Thompson, *J Electrochem Soc*, 2010, **157**, C18-C23.
- F. Mansfeld, *Corrosion*, 1976, **32**, 143-146.
- A. Usobiaga, A. de Diego and J. M. Madariaga, *Journal of Chemical & Engineering Data*, 2002, **48**, 81-85.
- N. Cabrera and N. F. Mott, *Reports on Progress in Physics*, 1949, **12**, 163-184.
- S. Ono, N. Kato, M. Saito and H. Asoh, in *Proceedings - Electrochemical Society*, 2006, pp. 34-42.
- W. Lee, R. Ji, U. Gosele and K. Nielsch, *Nat Mater*, 2006, **5**, 741-747.
- S. P. Albu, P. Roy, S. Virtanen and P. Schmuki, *Isr J Chem*, 2010, **50**, 453-467.
- S. So, K. Lee and P. Schmuki, *J Am Chem Soc*, 2012, **134**, 11316-11318.
- H. Habazaki, K. Fushimi, K. Shimizu, P. Skeldon and G. E. Thompson, *Electrochim Commun*, 2007, **9**, 1222-1227.
- K. Shimizu, K. Kobayashi, G. E. Thompson, P. Skeldon and G. C. Wood, *J Electrochem Soc*, 1997, **144**, 418-423.
- S. Berger, S. P. Albu, F. Schmidt-Stein, H. Hildebrand, P. Schmuki, J. S. Hammond, D. F. Paul and S. Reichlmaier, *Surface Science*, 2011, **605**, L57-L60.
- H. Habazaki, M. Uozumi, H. Konno, K. Shimizu, P. Skeldon and G. E. Thompson, *Corros Sci*, 2003, **45**, 2063-2073.
- M. E. StRauManis and P. C. Chen, *J Electrochem Soc*, 1951, **98**, 234-240.
- M. E. Straumanis, W. J. James and J. L. Ratliff, *Journal of the Less Common Metals*, 1961, **3**, 327-332.
- D. Kowalski and P. Schmuki, *Chemical Communications*, 2010, **46**, 8585-8587.

Journal Name

49. D. Kowalski and P. Schmuki, *Chemphyschem*, 2012, **13**, 3790-3793.
50. D. Kowalski, S. P. Albu and P. Schmuki, *Rsc Advances*, 2013, **3**, 2154-2157.